Impact of rise and fall phases of shear on platelet activation and aggregation using microfluidics

Xuemei Gao[1] · Tiancong Zhang[2] · Xiaojing Huang[1] · Xuanrong Huan[3] · Yuan Li[1]

Abstract

Blood flow disorders are often the result of the non-physiological narrowing of blood arteries caused by atherosclerosis and thrombus. The blood then proceeds through rising-peak-decreasing phases as it passes through the narrow area. Although abnormally high shear is known to activate platelets, the shear process that platelets undergo in small arteries is complex. Thus, understanding how each shear phase affects platelet activation can be used to improve antiplatelet therapy and decrease the risk of side effects like bleeding. Blood samples were sheared (68.8 ms, 5200 s^{-1}) in vitro by the microfluidic technique, and platelet activation levels (P-selectin and integrin $\alpha IIb\beta3$) and von Willebrand factor (vWF) binding to platelets were analyzed by flow cytometry. Post-stenosis platelet aggregation was dynamically detected using microfluidic technology. We studied TXA2, P2Y$_{12}$-ADP, and integrin $\alpha IIb\beta3$-fibrinogen receptor pathways by adding antiplatelet drugs, such as acetylsalicylic acid (ASA, an active ingredient of aspirin that inhibits platelet metabolism), ticagrelor (hinders platelet activation), and tirofiban (blocks integrin $\alpha IIb\beta3$ receptor) in vitro, respectively, to determine platelet activation function mediated by transient non-physiological high shear rates. We demonstrated that platelets can be activated under transient pathological high shear rates. The shear rise and fall phases influenced shear-induced platelet activation by regulating the binding of vWF to platelets. The degree of platelet activation and aggregation increased with multiple shear rise and fall phases. ASA did not inhibit shear-mediated platelet activation, but ticagrelor and tirofiban effectively inhibited shear-mediated platelet activation. Our data demonstrated that the shear rise and fall phases play an important role in shear-mediated platelet activation and promote platelet activation and aggregation in a vWF-dependent manner. Blocking integrin $\alpha IIb\beta3$ receptor and hindering P2Y$_{12}$-ADP were beneficial to reducing shear-mediated platelet activation.

Keywords Shear rise and fall phase · Von willebrand factor · Microfluidics · Platelet · Thrombosis

Introduction

Platelets play a crucial role in maintaining physiological hemostasis. However, pathological platelet aggregation can often lead to thrombosis within the body [1, 2]. Under normal physiological conditions, platelets bind to collagen fibers at the site of an injured endothelium and form clusters, resulting in platelet aggregation. Platelets accelerate the formation of clots at the site of injury by releasing substances such as ADP, TXA2, and thrombin, which promote blood coagulation, facilitating hemostasis. However, platelets can also form non-physiological aggregates under certain circumstances, leading to various cardiovascular diseases [3, 4]. For instance, atherosclerosis and vascular grafts often result in vascular stenosis and flow disturbances, such as pathological high shear gradients, which have been shown to increase platelet concentration near the vessel wall and activate platelets [5]. However, the mechanisms underlying shear-dependent platelet aggregation at sites of atherosclerotic stenosis remain poorly understood.

The primary mechanism driving shear-mediated platelet activation (SMPA) is the binding of von Willebrand factor

✉ Yuan Li
  liyuan_1985999@163.com

1   Central Laboratory of Yong-Chuan Hospital, Chongqing Medical University, Chongqing, China

2   Department of Laboratory, West China Hospital, Sichuan University, Sichuan, China

3   Department of Clinical Laboratory of Yong-Chuan Hospital, Chongqing Medical University, Chongqing, China

(vWF) to the platelet surface glycoprotein Ibα (GPIbα) [6]. Stretching vWF at high shear rates exposes the A1 binding site, which then binds with GPIbα to activate platelets and initiate intracellular signaling pathways. This process includes the release of Ca^{2+}, actin polymerization, cytoskeleton reorganization, signal protein phosphorylation, and integrin αIIbβ3 activation. The attachment of integrin αIIbβ3 to fibrinogen leads to stable adhesion. Endogenous chemical agonists like adenosine diphosphate (ADP) and thromboxane A2 (TXA2) are released by activated platelets, which further enhances platelet activation and contributes to the development of thrombosis [7, 8]. High shear rates can also cause mechanical damage to platelets, leading to their dissolution and the release of thromboplastin. This further exacerbates the risk of thrombosis. Activated platelets can also play a role in inflammation by binding to the leukocyte receptor P-selectin glycoprotein ligand-1 (PSGL-1) through P-selectin (CD62P) expressed on their surface. This interaction between platelets and leukocytes contributes to the complex interplay between the immune and coagulation systems [9]. These systems collaborate in a complex anti-infection process. The soluble form of P-selectin in plasma strengthens the relationship between inflammation, thrombosis, and coagulation at the site of vascular injury. P-selectin is highly expressed in inflamed plaques in atherosclerosis [10, 11]. Platelet-derived microparticles (PDMPs) can be driven by shearing and affect inflammation and blood coagulation. Shear-induced PDMPs prevent platelet aggregation driven by collagen or ADP but promote the production of thrombin [12, 13].

When stenosis occurs, platelets undergo rapid acceleration, persistence, and deceleration shear phases over a short period [14]. The effects of each phase on adhesion, aggregation, and platelet activation are different. Previous studies reported that shear exposure duration and shear values significantly impacted platelet adhesion, aggregation, and activation. The behavior of adhesion and aggregation in narrow areas was also affected by changes in hemodynamics, the vessel wall, and alterations in the thrombogenic potential of blood [15–17]. Platelets can be efficiently activated by high shear. However, how shear acceleration and deceleration phases affect platelet activation and aggregation remain poorly defined. Thus, further investigating whether the shear rise and fall phases affect platelet activation when exposed to high shear at the same time would be beneficial. A better understanding of the precise regulation of thrombus formation in atherosclerotic vessel segments is critical for improving current antithrombotic treatments. A full understanding of the effect of the shear rise and fall phase on platelet activity will be beneficial to preventing and treating cardiovascular diseases.

The development of micro- and nanotechnology has enabled explorations into the relationship between platelets and plasma proteins under conditions close to physiological flow using microfluidic micro-array technology. A microchannel with a certain narrow area can mimic the high shear of a stenotic microenvironment in vitro and provide the shear values needed in the experiments [18]. The adhesion and aggregation behavior of platelets in the channel can be observed and analyzed immediately. Therefore, microchannel models with the same total narrow length but different segments were used in this study to explore the effect of the shear rise and fall phases on platelet activation in vitro.

Methods

Design and processing of microfluidic chip

The microfluidic chip was processed using the dry photosensitive film soft lithography process reported by our research group [19]. Different from the liquid photoresist used in the traditional soft lithography process, dry photosensitive film has the advantages of low cost and no need for an expensive clean space or professional lithography equipment. Therefore, it is easier to use in general biology and medical laboratories. More importantly, the depth of the microchannel structure can be controlled more accurately than liquid photoresist (the thickness is controlled by the spin speed) because commercial dry photosensitive film has a fixed thickness. The microfluidic chip has 6 microchannels. The microchannel length is 7 mm, the width is 1 mm, and the height is 0.07 mm. The microchannel is narrowed by 80% at the center, with a total stenotic length of 4 mm. The experimental setup provided the same high shear rate time but different stenotic segments, resulting in different shear gradient times. The physiological shear rates were set as the pre-stenosis shear environment. The simple process was as follows. The chip mask pattern was designed by Coreldraw12.0 software (Corel, Canada) and printed on transparent film by an inkjet printer to make a mask. A 2-layer dry photosensitive film (single layer thickness of 35 μm) was laminated on a copper plate using a laminating machine, and ultraviolet rays were passed through the mask to irradiate the dry photosensitive film. The chip-positive film was developed by soaking it in a 1% sodium carbonate solution. A prepolymer made from a mixture of a polydimethylsiloxane (PDMS) matrix and a curing agent at a 10:1 ratio (m/m) was poured onto the chip-positive film, vacuumed, and cured at 60 °C for 3 h. The cured PDMS substrate was stripped from the dry photosensitive positive film, and sample pools and outlets with diameters of 7 and 1.5 mm were punched using a flat-end punch. After

treatment with an oxygen plasma cleaning machine (30 W for 1 min), the cured PDMS was irreversibly bonded to a cleaned glass slide to form a glass microfluidic chip. A chip sketch and schematic diagram of the microfluidic operation are shown in Fig. 1.

Blood collection and treatment

The study was approved by the Ethics Committee of Yongchuan Hospital affiliated with Chongqing Medical University and informed consent was obtained before blood collection. Experimental blood samples were collected from 12 healthy adult volunteers. The volunteers had no history of taking medicine within 2 weeks. Venous blood samples were anticoagulated with 3.2% sodium citrate at a 1:9 ratio (v / v), stored at room temperature, and used within 2 h. A total of 4 experience indicators (the platelet aggregation index in microfluidic channels, two platelet activation indexes in flow cytometry, and vWF binding to platelets index in flow cytometry) were tested 12 times in different donor blood samples. Shear-induced platelet activation (expression of P-selectin and Integrin $\alpha_{IIb}\beta_3$) and aggregation were studied in whole blood samples, and shear-induced monocyte-platelet aggregation was studied in lysed erythrocytes from whole blood. Whole blood was incubated with 1 mL of 1× erythrocyte lysate (BD Biosciences, USA) at room temperature for 10 min to lyse red blood cells and centrifuged at 450 g for 5 min. Platelet sediment at the bottom was retained, washed, and resuspended in phosphate-buffered saline PBS (Bio-Channel, China). The binding of vWF to platelets was studied using platelet-rich plasma (PRP). Whole blood was centrifuged at 200 g for 10 min, and the supernatant was collected as PRP.

Microchannel fluid simulation

The shear rate of blood flow in capillaries has been reported to be between 500 and 5000 s^{-1} in the absence of contraction [20]. We set the outlet flow to 50 uL/min and the inlet to hydrostatic pressure so that the input shear rate was 1000 s^{-1} to simulate in vivo hemodynamics. The peak shear rate at the stenosis was 5200 s^{-1}, which reached the pathological high shear level. The structure of the microchannel was designed by SolidWorks software (Dassault Systems, USA), and the wall shear rate (WSR)
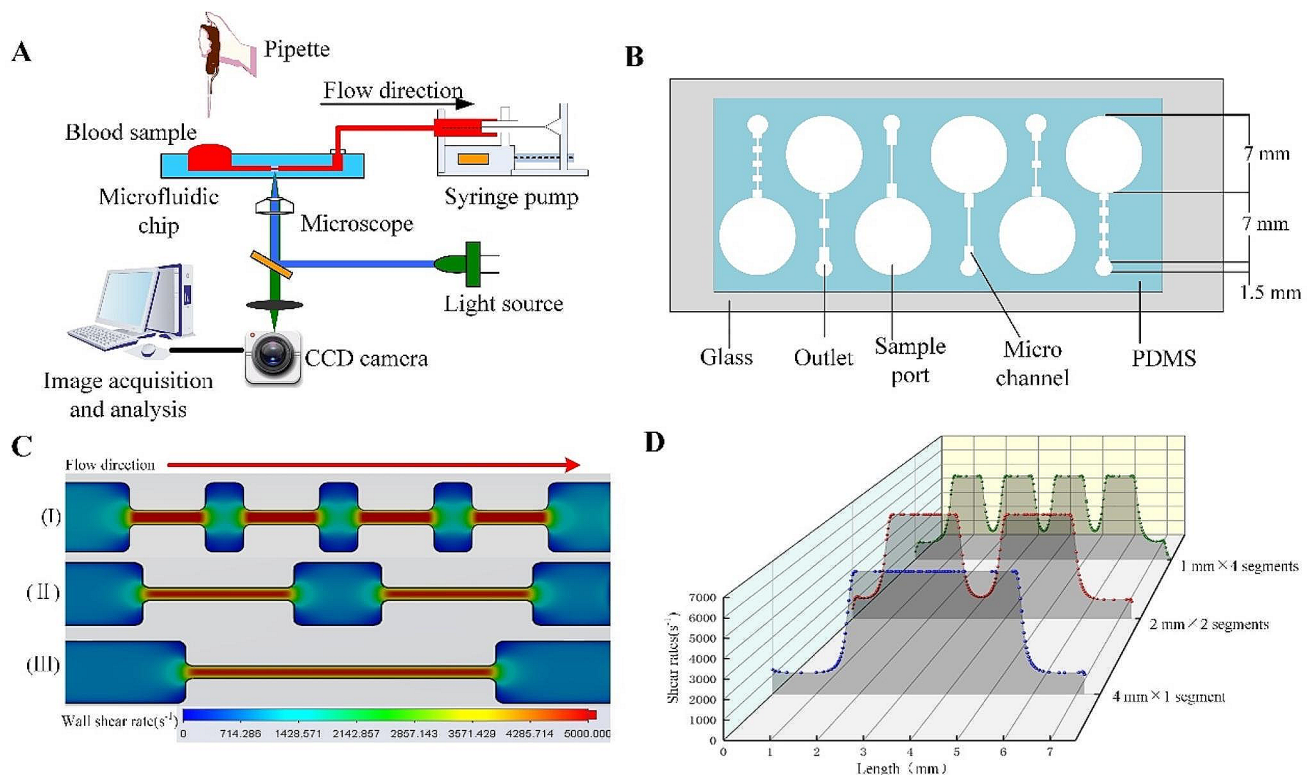

Fig. 1 Microfluidic chip analysis system and CFD simulations within narrow microchannels. (A) Schematic diagram of the microfluidic chip. (B) Flowchart of the microfluidic chip analysis system. (C) Wall shear rate distribution with dark blue indicating minimum values and dark red indicating maximum values. (I), (II) and (III) represent narrow lengths of 1 mm × 4 segments, 2 mm × 2 segments, and 4 mm × 1 segment, respectively. (D) History of shear rate changes experienced by platelets moving along the midline of the microchannel floor as predicted by CFD simulations. The shear rate increased with vessel narrowing, and particles in the flow line underwent rapid shear rate acceleration, persistence, and deceleration phases over a short time (68.8 ms). CFD, computational fluid dynamics

distribution in the microchannel was simulated by computational fluid dynamics (CFD) through its fluid simulation module (flow simulation). The fluid properties were assumed to be stable with incompressible laminar flow. A total of 85,630 grids were created inside the model, and the CFD solution converged to a resulting reduction of 6 orders of magnitude in 165 iterations through a solver operation.

Platelet aggregation studies at post-stenotic sites

A 1 mg/ mL fibrinogen solution ($\geq 80\%$ of the protein was cuttable, MerckKGaA, GER) was perfused into the microfluidic channel and incubated at 37 °C for 1 h for uniform adsorption to the bottom of the channel before conducting the experiments. Uncoated areas were blocked with 3% bovine serum albumin (BSA, Ortho, USA). After 1 h, the microchannel was rinsed with PBS. Calcein AM (Invitrogen, USA) is a live cell fluorescent dye that can penetrate the cell membrane and enter cells, then is sheared by intracellular esterase to form calcein. It emits strong green fluorescence and enables the fluorescent labeling of platelets in blood samples. The fluorescently labeled whole blood sample was added to the sample pool, and a syringe pump was used to control the flow of blood in the microchannel at a set shear rate. The camera was controlled by Streampix 5.0 (Norpix, Canada) software to record the aggregation behavior of fluorescently labeled platelets in the microchannel at a speed of 1 frame/1s (objective ×20). One hundred and twenty sequential fluorescence images were recorded for 2 min. Coverage analysis of the acquired sequences was performed by ImageJ (NIH, USA).

Platelet activation

Shear-induced platelet activation was analyzed by flow cytometry (Beckman Coulter, USA). Freshly collected sodium citrate anticoagulated blood was used immediately (to avoid in vitro activation). The microchannel was blocked with 3% BSA for 1 h before whole blood perfusion, and then the microchannel was washed with PBS. The whole blood was injected into the sample pool and collected from the microchannel. A 5 uL sample of collected blood was added to a centrifuge tube with 25 uL of 0.5% BSA and 5 uL of PerCP-eFluor710-labeled CD61(eBioscience, USA), 5 uL of FITC-labeled PAC-1 (eBioscience), and 5ul of PE-labeled CD62P (eBioscience) were added and incubated for 20 min at room temperature in the dark. The sample was fixed by adding 1 mL of 1% paraformaldehyde (Biyuntian Biotechnology Company, China). Unstimulated whole blood was used

as the negative control. The platelet population was identified by CD61 monoclonal antibody positivity. Finally, the expression levels of CD62P and PAC-1 on the surface of individual platelets were measured. Platelet aggregation was expressed as the percentage of CD61 intensity. CytExpert software (Beckman Coulter, USA) was used to collect and analyze the data for 10,000 events.

In this experiment, platelet activation studies at different shear rise and fall times (1 mm × 4, 2 mm × 2, and 4 mm × 1) and in vitro inhibition studies were performed at 5200 s^{-1} (the pre-stenotic and post-stenotic shear rates were 1000 s^{-1}). ASA, ticagrelor, and tirofiban can effectively inhibit shear-induced platelet aggregation in vitro. ASA reduces the synthesis of prostaglandins and thromboxane by inhibiting cyclooxygenase (COX) to reduce thrombosis. Ticagrelor reversibly inhibits the platelet P2Y$_{12}$ receptor and blocks ADP stimulation on platelets. Tirofiban specifically inhibits the binding of integrin αIIbβ3 to fibrinogen, the last step of platelet aggregation in the activation process. ASA, ticagrelor, and tirofiban inhibition were investigated at the recommended concentration of 2 μM.

vWF binds to platelets

CD41-stained platelets and CD61-stained platelets can bind to vWF as vWF is stretched. CD41/ CD61-positivity can characterize binding between vWF and platelets. Washed platelets with single-stain fluorescence were prepared. PRP was stained with anti-CD61/PerCP-eFluor710 and anti-CD41/PE/Ab for 20 min at room temperature in the dark, then washed twice with Tyrode's Solution (Procell Life Science & Technology Co., Ltd.), resuspended with platelet-poor plasma (PPP), quantified to 3×10^8 platelets/mL, and stored away from light. Shear platelet samples were prepared by mixing equal proportions of stained platelets and PPP. An unstimulated platelet sample was tested immediately as a negative control. The experimental samples were collected in a centrifuge tube after shearing. CytExpert software was used to collect and analyze the data for 10,000 events.

Data analysis

All experiments were repeated at least 3 times, and values are expressed as the mean ± standard deviation (mean ± SD). Differences between groups were analyzed by one-way ANOVA and Tukey's post hoc test. The data were analyzed using GraphPad 9.0 software (GraphPad Software, USA).

Results

The narrow length in the microfluidic chip is the same, but the rise and fall phase times are different

A CFD simulation was conducted to analyze the fluid shear of platelets flowing through the microfluidic chip. The shear rate distribution in the microchannels with 80% stenosis was the same, but the microchannels had different segmental stenoses (Fig. 2). We found that the shear rates in the narrow channel increased, leading to a gradient change in the WSR. We analyzed the WSR distribution of streamlines at the bottom of the microchannels to determine the changes in platelet shear rates in the microchannels further. When the input shear rate on the linear microchannel was $1000\ s^{-1}$, the WSR distribution was uneven in the narrow channel, and the maximum WSR reached $5200\ s^{-1}$ (Fig. 2B). At an input shear rate of $1000\ s^{-1}$, platelets flowed through the narrow channel, experienced a transient increase and

decrease in shear rates in a very short time (68.8 ms), and finally returned to the input shear rates. The platelets experienced multiple shear rate increases and decreases as the number of narrow segments increased.

Differences in platelet activation levels

P-selectin is an internal protein of α-granule membranes. During exocytosis, due to the fusion of α-granules and the external platelet plasma membrane, granules appear on the platelet surface after platelet activation. In our study, P-selectin exposure was detected by flow cytometry. Platelets with high fluorescence intensity (fluorescence intensity 1×10^{3}) were selected as the P-selectin-positive population. The peak fluorescence intensity shifted to the right with increases in the number of P-selectin-positive platelets (% of platelets), indicating an increase in P-selectin exposure. The degree of platelet activation was significantly different among the four different stenotic segment models, and the
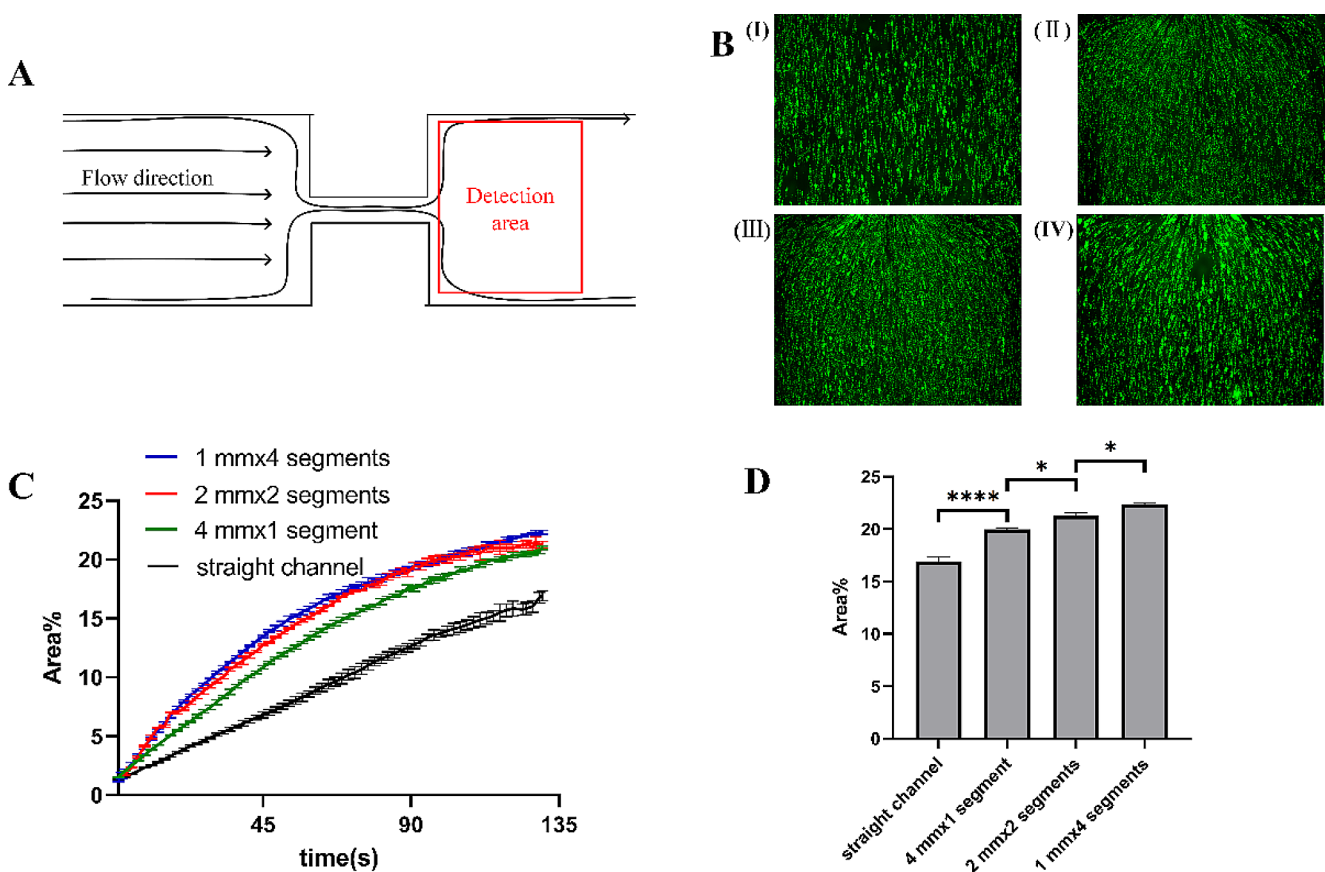

Fig. 2 Platelet aggregation on fibrinogen under dynamic conditions. (A) Schematic representation of the platelet detection area. (B) Fluorescence images of platelet aggregation occurring on the fibrinogen surface. (I), (II), (III), and (IV) represent straight channels and groups with narrow lengths of 4 mm × 1 segment, 2 mm × 2 segments, and 1 mm × 4 segments, respectively. Green fluorescent spots are platelet aggregates. (C) The curve of the relationship between platelet cover-age and flow time on the fibrinogen surface of the microchannels. (D) Platelet aggregation coverage at 120 s. The independent experimental data of 3 different donors were summarized, and the mean (M) ± standard deviation (SD) as error bars were plotted. P-values were calculated vs. straight channel platelet aggregation by one-way analysis of variance (ANOVA); *$p \leq 0.05$, ****$p \leq 0.0001$

degree of platelet activation in the four models was significantly different from that of resting platelets ($P < 0.0001$). At a fixed exposure time, the expression of P-selectin increased with shear rise and fall increases (Fig. 3B).

The activation of integrin $\alpha_{IIb}\beta_3$ is a key step in platelet aggregation and thrombosis. The activation is due to a conformational change in the cytoplasmic domain of the GP complex, which leads to a significant increase in adhesion to the protein-ligand fibrinogen and vWF, resulting in platelet aggregation. We quantified and compared the number of all integrin $\alpha_{IIb}\beta_3$-positive platelets to measure the degree of $\alpha_{IIb}\beta_3$ activation. Among CD61-positive platelets, those with PAC-1 positivity were distinguished according to their fluorescence intensity (fluorescence intensity 3×10^3) and defined as activated $\alpha_{IIb}\beta_3$. We found that integrin $\alpha_{IIb}\beta_3$ could be activated under transient high shear. The number of activated integrin $\alpha_{IIb}\beta_3$ platelets in the shear-treated groups increased significantly compared to resting platelets ($P \leq 0.001$). The activated integrin $\alpha_{IIb}\beta_3$ platelet count and fluorescence intensity increased. The expression of PAC-1

increased in the microchannels with multiple narrow segments at a fixed exposure time (Fig. 3C).

vWF binding to platelets is the key to the SMPA rise and fall phases

SMPA is mediated by the binding of vWF to the platelet membrane protein GPIbα. When vWF binds to platelets, an activation cascade occurs in cells, leading to further adhesion and the aggregation of platelets. The CD41/CD61 platelet count was analyzed to determine the degree of binding between vWF and platelets. The binding of soluble vWF to platelets (Q2-UR) was increased in multiple narrow segments (Fig. 4).

The inhibition of SMPA by antiplatelet drugs is different

ASA is an antiplatelet agent that irreversibly inhibits COX-1 activity and reduces the conversion of arachidonic acid

Fig. 3 Shear-induced platelet activation (P-selectin exposure and αIIbβ3 integrin activation). Whole blood samples were exposed to 5200 s^{-1} in 68.8 ms. A and C: Representative peak diagrams of the fluorescence intensity distribution in platelets. B and D: Positive platelet counts. The independent experimental data from 5 different donors were summarized, and the mean (M) ± standard deviation (SD) as error bars were plotted. P-values were calculated vs. intact platelets by one-way analysis of variance (ANOVA); *$p < 0.05$, **$p < 0.01$, ****$p \leq 0.0001$
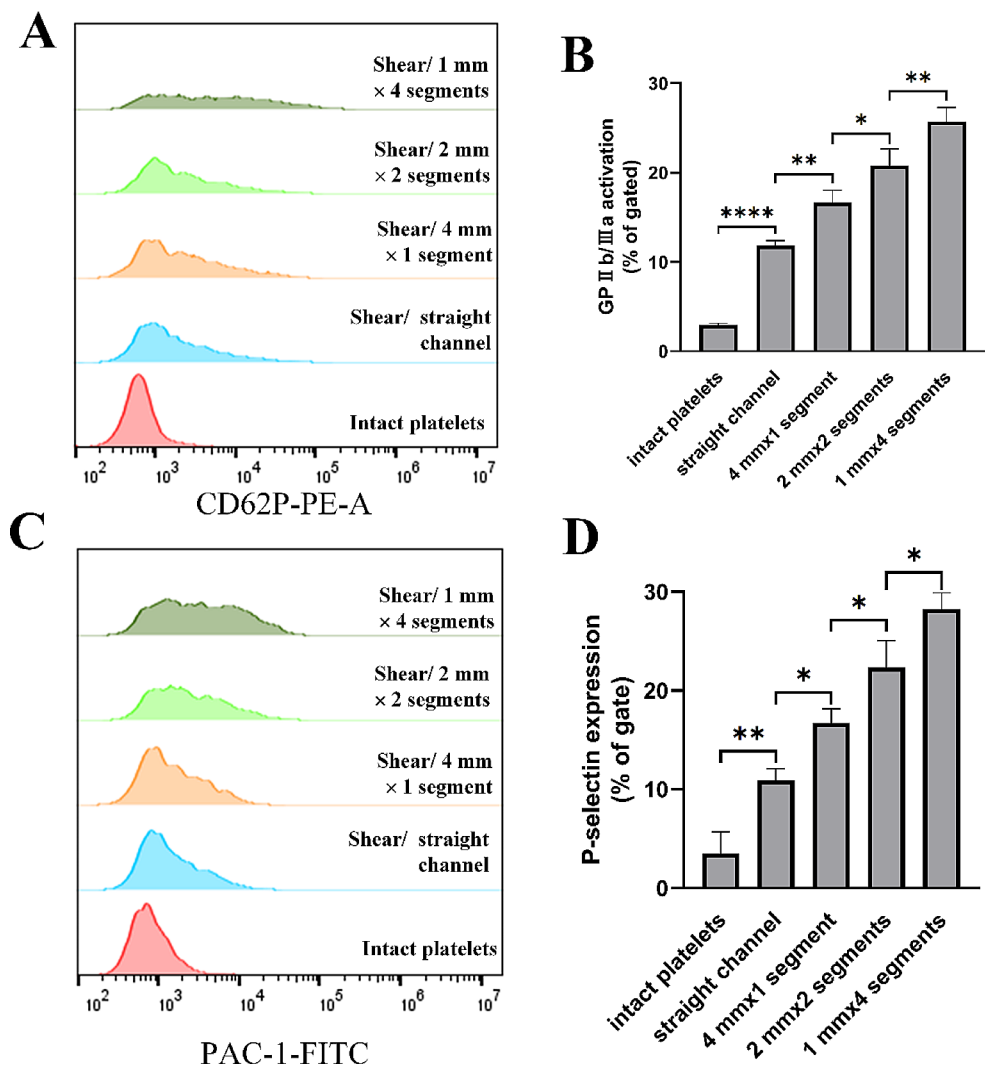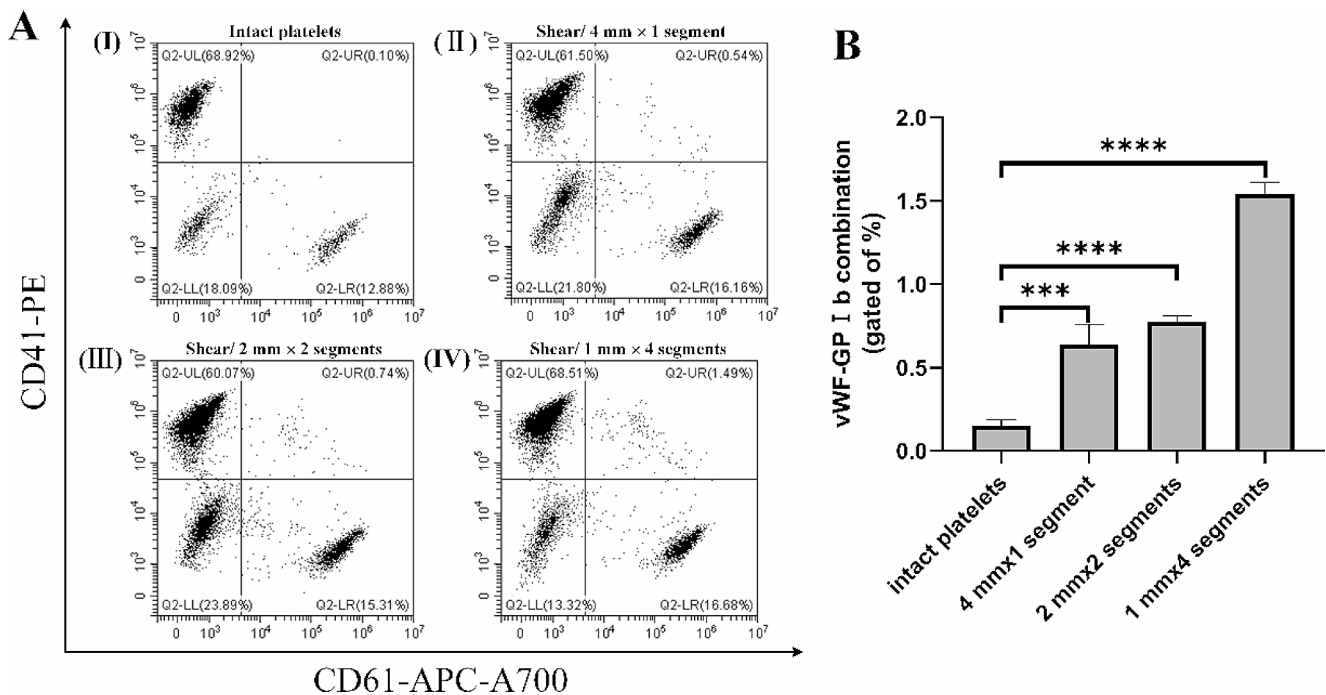
Fig. 4 The shear rise and fall phases exacerbate the binding between vWF and platelets. Whole blood samples were exposed to shear rates utilizing narrow microchannels at 5200 s^{-1} in 68.8 ms. (A) Representative flow scatter diagram. (B) Count of platelets binding by vWF. The independent experimental data from 5 different donors were summarized, and the mean (M) ± standard deviation (SD) as error bars were plotted. P-values were calculated vs. intact platelets by one-way analysis of variance (ANOVA); ***$p \leq 0.001$, ****$p \leq 0.0001$

(AA) to thromboxane A2 (TXA2). Our results showed that ASA had a little inhibitory effect on shear-induced platelet activation (Fig. 5), indicating that the TXA2 activation pathway is not a major pathway in shear-induced platelet activation. Platelet P-selectin and GPIIb/IIIa expression levels were significantly reduced after ticagrelor inhibition, suggesting that the ADP- P2Y12 receptor pathway is partially involved in shear-induced platelet activation (Fig. 5). Tirofiban inhibits platelet aggregation by competitively binding to fibrinogen receptors GPIIb/IIIa. In the present study, tirofiban significantly inhibited the expression of GPIIb/IIIa, suggesting that the binding of platelet GPIIb/IIIa to fibrinogen is not only the ultimate pathway for platelet aggregation but also has a non-negligible effect on shear-induced platelet activation. The schematic figure of the study is shown in Fig. 6. By comparing the levels of platelet adhesion, aggregation, and activation in different microchannels, determine the impact of shear rise and fall in shear-induced platelet activation.

Discussion

SMPA can occur under pathological high-shear conditions. Pathological high shear conditions can occur from atherosclerosis or vascular stent implantation [21]. The most commonly used mechanical circulation support (MCS) devices in the clinic include a ventricular assist device, a pump oxygenator for extracorporeal membrane oxygenation, and a heart-lung machine for cardiopulmonary bypass. The clinical application of MCS provides important perfusion for all organs and maintains their function [22, 23]. However, when medical devices are implanted into blood vessels, stenoses sometimes form in the anastomotic area of vascular grafts or along the inner wall of the graft due to intimal fiber hyperplasia at local sutures. A transient high-shear environment occurs in narrow areas, increasing the risk of thrombosis.

High shear promotes platelet activation, and the platelet response is different under different shear stresses. SMPA is mainly mediated by the binding of vWF to GPIbα. Under high shear, vWF is stretched and exposed so that site A1 binds to GPIbα [24]. Then, an activation cascade occurs in platelets, including platelet protein phosphorylation, calcium release, cytoskeleton protein contraction, and vesicle release. Released chemical agonists, such as ADP, can activate the surrounding platelets and amplify platelet activation. Finally, platelets bind to fibrinogen through activated $\alpha_{IIb}\beta_3$ to form stable aggregates.

Pathological high shear consists of instantaneous elevated, peak, and instantaneous decreasing phases. These 3 phases have different effects on platelet activation and are worth exploring carefully because previous experiments showed that platelet aggregation behavior was regulated by hemodynamics; platelets gather in the shear decline area

Fig. 5 Effect of different inhibitors on platelet activation. A and C: Expression of P-selectin and PAC-1. The results are shown as superimposed histograms. B and D: P-selectin and PAC-1 expression statistics. Results are shown as the mean ± standard deviation. *$p < 0.05$, ** $p < 0.01$, ***$p < 0.001$
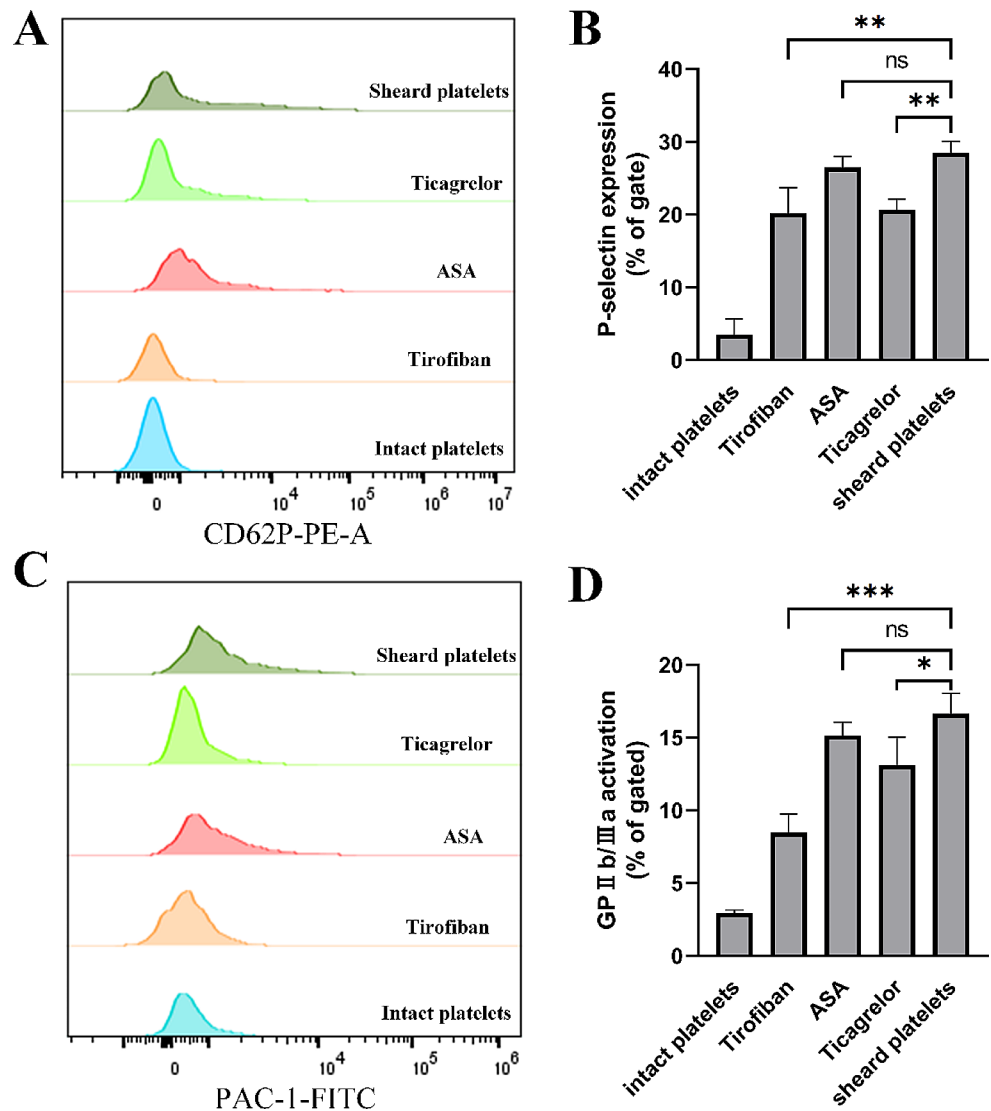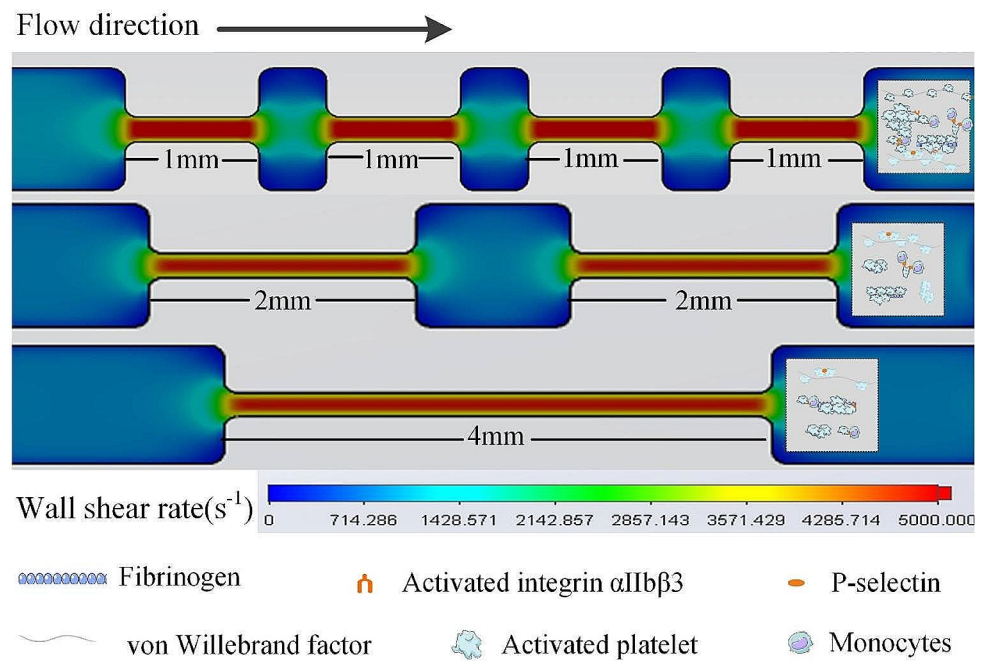
first and are mainly stable downstream from the stenosis. The shape and degree of narrowing are factors that determine the shear environment [25]. The shear rate of a small vein and a large vein is lower than 500 s^{-1}, and the shear rate of a small artery can reach 5000 s^{-1}. When the degree of stenosis exceeds 70%, the shear rate will rise sharply. For example, when the initial shear rate is 1000 s^{-1}, the shear can increase to 14,700 s^{-1}.

A previous study showed that vWF is very sensitive to shear [26]. It can be stretched under high shear in 10 ms. However, the stretching of vWF is reversible, which can reduce the risk of thrombosis in the human body [27]. Pathological high shear mediates platelet activation through vWF. Thus, we explored whether the shear rise and fall phases could promote the binding of vWF to platelets and platelet activation. The microfluidic technique was used to simulate pathological stenotic vessels in vitro to produce different shear rise and fall phase times. The total stenotic length was

4 mm to ensure a high shear exposure time of 68.8 ms. The experimental results suggest that every time platelets experience increases and decreases in shear, they will aggregate. A high shear rate stretches vWF, but the binding force between vWF and platelets is not enough to resist shear stress resistance, and the shear decrease phase is conducive to better binding. Elevating and descending shear phases are beneficial to the binding of platelets to vWF, and the activation and aggregation of platelets will also increase. Although not a large quantity of platelets will bind to vWF, the activation level of platelets is high. Considering the lack of an anticoagulation system in vitro, platelet activation showed a positive feedback accumulation effect. We also believe that the smoothness of the implant surface will affect SMPA to a certain extent. A smoother implant surface can lower the risk of platelet activation. However, further research is needed to investigate that hypothesis. The high shear that platelets

Fig. 6 Visual abstract. Summary scheme graphic showing the platelet activation and aggregation levels at the post-stenotic area between different narrow segments microchannels. The narrow length is a total of 4 mm, but the rise and fall phases are different in each microchannel. The shear rise and fall phases are beneficial to platelet activation and aggregation

Flow direction

1mm 1mm 1mm 1mm

2mm 2mm

4mm

Wall shear rate(s⁻¹) 0 714.286 1428.571 2142.857 2857.143 3571.429 4285.714 5000.000

oooooooo Fibrinogen ⋂ Activated integrin αIIbβ3 ▬ P-selectin

⌒ von Willebrand factor Activated platelet Monocytes

experience in vivo is due to circulatory factors, which may have a certain impact on platelet activation.

Antiplatelet therapy is an important strategy for the clinical prevention and treatment of postoperative thrombosis in cardiovascular diseases such as stent implantation. The balance between thrombus and bleeding risk is a major problem in antiplatelet therapy. Antiplatelet drugs should be used according to the condition of the patient. Other antiplatelet drugs can also be used in monoclonal antibody platelet therapy according to the patient's risk of ischemia and bleeding and the route of treatment [28]. Dual antiplatelet therapy with aspirin + clopidogrel/ticagrelor is commonly used. Clinical evidence suggests that the combination of clopidogrel and aspirin can further reduce the risk of thrombotic events in patients with coronary heart disease and stent implantation compared with aspirin alone after percutaneous coronary intervention [29]. In this study, aspirin showed a trend to inhibit shear-induced platelet activation, but it lacked statistical significance, consistent with previous studies. Ticagrelor and tirofiban effectively inhibited shear-induced platelet activation, which is consistent with clinical use. The findings have certain reference significance for the prevention of thrombus in pathological stenosis.

Conclusion

Here, we demonstrated that platelets can be activated under transient pathological high shear, which increases the risk of thrombosis. The shear rise and fall phases are beneficial to platelet activation and may regulate platelet activation by promoting vWF binding to platelets.

Limitations

The recovery distance experienced by the shear gradient was not long enough, and the shear rate continued to rise before falling to the base values, which may have made the rise and fall phases not obvious enough.

Relationship Disclosure

None of the authors have any relationships relevant to this paper to disclose.

References

1. Meijden. PEJvd, Heemskerk JWM (2019) Platelet biology and functions: new concepts and clinical perspectives. Nat Rev Cardiol 16(3):166–179. https://doi.org/10.1038/s41569-018-0110-0

2. Dib PRB, Quirino-Teixeira AC, Merij LB, Pinheiro MBM, Rozini SV, Andrade FB, Hottz ED (2020) Innate immune receptors in platelets and platelet-leukocyte interactions. J Leukoc Biol 108(4):1157–1182. https://doi.org/10.1002/jlb.4mr0620-701r

3. Ding J, Chen Z, Niu S, Zhang J, Mondal NK, Griffith BP, Wu ZJ (2015) Quantification of Shear-Induced platelet activation: high shear stresses for short exposure time. Artif Organs 39(7):576–583. https://doi.org/10.1111/aor.12438

4. Chen Z, Koenig SC, Slaughter MS, Griffith BP, Wu ZJ (2018) Quantitative characterization of Shear-Induced platelet receptor shedding: glycoprotein ibalpha, glycoprotein VI, and glycoprotein IIb/IIIa. ASAIO J 64(6):773–778. https://doi.org/10.1097/MAT.0000000000000722

5. Al-Tamimi M, Tan CW, Qiao J, Pennings GJ, Javadzadegan A, Yong AS, Arthur JF, Davis AK, Jing J, Mu FT, Hamilton JR, Jackson SP, Ludwig A, Berndt MC, Ward CM, Kritharides L, Andrews RK, Gardiner EE (2012) Pathologic shear triggers shedding of vascular receptors: a novel mechanism for downregulation of platelet glycoprotein VI in stenosed coronary vessels. Blood 119(18):4311–4320. https://doi.org/10.1182/blood-2011-10-386607

6. Maxwell MJ, Westein E, Nesbitt WS, Giuliano S, Dopheide SM, Jackson SP (2007) Identification of a 2-stage platelet aggregation process mediating shear-dependent thrombus formation. Blood 109(2):566–576. https://doi.org/10.1182/blood-2006-07-028282

7. Hanke J, Ranke C, Perego E, Koster S (2019) Human blood platelets contract in perpendicular direction to shear flow. Soft Matter 15(9):2009–2019. https://doi.org/10.1039/c8sm02136h

8. Sang Y, Roest M, De Laat B, De Groot PG, Huskens D (2021) Interplay between platelets and coagulation. Blood Rev 46100733. https://doi.org/10.1016/j.blre.2020.100733

9. Mariscal A, Zamora C, Magallares B, Salman-Monte TC, Ortiz MA, Diaz-Torne C, Castellvi I, Corominas H, Vidal S (2021) Phenotypic and functional consequences of PLT binding to Monocytes and its association with clinical features in SLE. Int J Mol Sci 22(9). https://doi.org/10.3390/ijms22094719

10. Pluta K, Porebska K, Urbanowicz T, Gasecka A, Olasinska-Wisniewska A, Targonski R, Krasinska A, Filipiak KJ, Jemielity M, Krasinski Z (2022) Platelet-leucocyte aggregates as novel biomarkers in Cardiovascular diseases. Biology (Basel) 11(2). https://doi.org/10.3390/biology11020224

11. Bester J, Pretorius E (2016) Effects of IL-1beta, IL-6 and IL-8 on erythrocytes, platelets and clot viscoelasticity. Sci Rep 632188. https://doi.org/10.1038/srep32188

12. Slepian MJ, Sheriff J, Hutchinson M, Tran P, Bajaj N, Garcia JGN, Scott Saavedra S, Bluestein D (2017) Shear-mediated platelet activation in the free flow: perspectives on the emerging spectrum of cell mechanobiological mechanisms mediating cardiovascular implant thrombosis. J Biomech 5020–5025. https://doi.org/10.1016/j.jbiomech.2016.11.016

13. Gidaro A, Delitala AP, Manetti R, Caccia S, Soloski MJ, Lambertenghi Deliliers G, Castro D, Donadoni M, Bartoli A, Sanna G, Bergamaschini L, Castelli R (2023) Platelet microvesicles, inflammation, and coagulation markers: a pilot study. Hematol Rep 15(4):684–695. https://doi.org/10.3390/hematolrep15040069

14. Lui M, Gardiner EE, Arthur JF, Pinar I, Lee WM, Ryan K, Carberry J, Andrews RK (2019) Novel stenotic microchannels to study Thrombus formation in Shear gradients: influence of Shear forces and Human platelet-related factors. Int J Mol Sci 20(12). https://doi.org/10.3390/ijms20122967

15. Bark DL Jr. DNK (2010) Wall shear over high degree stenoses pertinent to atherothrombosis. J Biomech 43(15):2970–2977. https://doi.org/10.1016/j.jbiomech.2010.07.011

16. Kamada H, Imai Y, Nakamura M, Ishikawa T, Yamaguchi T (2017) Shear-induced platelet aggregation and distribution of thrombogenesis at stenotic vessels. Microcirculation 24(4). https://doi.org/10.1111/micc.12355

17. Jesty J, Yin W, Perrotta P, Bluestein D (2003) Platelet activation in a circulating flow loop: combined effects of shear stress and exposure time. Platelets 14(3):143–149. https://doi.org/10.1080/0953710031000092839

18. Rahman SM, Hlady V (2021) Microfluidic assay of antiplatelet agents for inhibition of shear-induced platelet adhesion and activation. Lab Chip 21(1):174–183. https://doi.org/10.1039/d0lc00756k

19. Zhang T, Liu L, Huang X, Gao X, Chen D, Huan X, He C, Li Y (2022) Application of microfluidic chip technology to study the inhibitory effect of tetramethylpyrazine on platelet aggregation, activation, and phosphatidylserine exposure mediated by pathological high shear rate. Blood Coagul Fibrinolysis 001–14. https://doi.org/10.1097/MBC.0000000000001179

20. Frojmovic MM (1998) Platelet aggregation in flow: Differential roles for adhesive receptors and ligands. Am Heart J 135:S119–S131 ((5 Pt 2 Su))

21. Rahman SM, Hlady V (2019) Downstream platelet adhesion and activation under highly elevated upstream shear forces. Acta Biomater 91(0):135–143. https://doi.org/10.1016/j.actbio.2019.04.028

22. Chen Z, Mondal NK, Ding J, Koenig SC, Slaughter MS, Wu ZJ (2016) Paradoxical effect of Nonphysiological Shear Stress on platelets and von Willebrand Factor. Artif Organs 40(7):659–668. https://doi.org/10.1111/aor.12606

23. Chen Z, Zhang J, Li T, Tran D, Griffith BP, Wu ZJ (2020) The impact of shear stress on device-induced platelet hemostatic dysfunction relevant to thrombosis and bleeding in mechanically assisted circulation. Artif Organs 44(5):1–13. https://doi.org/10.1111/aor.13609

24. Shida Y, Swystun LL, Brown C, Mewburn J, Nesbitt K, Danisment O, Riches JJ, Hough C, Lillicrap D (2019) Shear stress and platelet-induced tensile forces regulate ADAMTS13-localization within the platelet thrombus. Res Pract Thromb Haemost 3(2):254–260. https://doi.org/10.1002/rth2.12196

25. Bark DL Jr., Para AN, Ku DN (2012) Correlation of thrombosis growth rate to pathological wall shear rate during platelet accumulation. Biotechnol Bioeng 109(10):2642–2650. https://doi.org/10.1002/bit.24537

26. Liu ZL, Bresette C, Aidun CK, Ku DN (2022) SIPA in 10 milliseconds: VWF tentacles agglomerate and capture platelets under high shear. Blood Adv 6(8):2453–2465. https://doi.org/10.1182/bloodadvances.2021005692

27. Schneider SW, Nuschele S, Wixforth A, Gorzelanny C, Alexander-Katz A, Netz RR, Schneider MF (2007) Shear-induced unfolding triggers adhesion of Von Willebrand factor fibers. Proc Natl Acad Sci U S A 104(19):7899–7903. https://doi.org/10.1073/pnas.0608422104

28. Koo B-K, Kang J, Park KW, Rhee T-M, Yang H-M, Won K-B, Rha S-W, Bae J-W, Lee NH, Hur S-H, Yoon J, Park T-H, Kim BS, Lim SW, Cho YH, Jeon DW, Kim S-H, Han J-K, Shin E-S, Kim H-S, Koo B-K, Kang J, Park KW, Rhee T-M, Lee H, Yang H-M, Won K-B, Rha S-W, Bae J-W, Lee NH, Hur S-H, Yoon J, Park T-H, Kim BS, Lim SW, Cho YH, Jeon DW, Kim S-H, Han J-K, Shin E-S, Kim H-S, Han K-R, Moon K-W, Oh SK, Kim U, Rhee M-Y, Kim D-I, Kim S-Y, Lee S-Y, Lee SU, Kim S-W, Kim SY, Jeon H-K, Cha KS, Jo S-H, Ryu JK, Suh I-W, Choi H-H, Woo S-I, Chae I-H, Shin W-Y, Kim D-K, Oh JH, Jeong MH, Kim YH (2021) Aspirin versus clopidogrel for chronic maintenance

monotherapy after percutaneous coronary intervention (HOST-EXAM): an investigator-initiated, prospective, randomised, open-label, multicentre trial. Lancet 397(10293):2487–2496. https://doi.org/10.1016/s0140-6736(21)01063-1

29. Luckie M, Khattar RS, Fraser D (2009) Non-cardiac surgery and antiplatelet therapy following coronary artery stenting. Heart 95(16):1303–1308. https://doi.org/10.1136/hrt.2008.161273